

Galaxy Zoo: Quenching timescales of group galaxies

R. J. Smethurst,¹ C. J. Lintott,¹ and the Galaxy Zoo team ^{*}

¹ *Oxford Astrophysics, Department of Physics, University of Oxford, Denys Wilkinson Building, Keble Road, Oxford, OX1 3RH, UK*

4 September 2016

ABSTRACT

The environment does cause quenching. But it's not the dominant mechanism. So says GZ + SDSS + GALEX + STARPY on group galaxies.

1 INTRODUCTION

There are many mechanisms which are proposed to cause quenching; including mergers (?), mass quenching (??), morphological quenching (?) and the environment of a galaxy.

The galaxy environment as a cause of quenching was proposed due to the correlation of both morphology (Dressler 1980) and the quenched galaxy fraction (?) with environmental density.

BUT does this correlation truly imply causation? Evidence from simulations (?) suggests that the environment may not be the dominant quenching mechanisms for galaxies. Perhaps the correlation of increased galaxy quenched fractions with environment is due to a combination of mergers, mass and morphological quenching. In denser environments, galaxies are more likely to encounter another galaxy in a merger scenario and large viral radii give rise to long infall times during which gas reservoirs can be depleted due to star formation.

To study this we need to look at how quenching timescale changes in groups and clusters of galaxies with different properties in order to isolate the cause of the density-morphology and density-SFR correlations.

2 DATA AND METHODS

2.1 Data Sources

In this investigation we use visual classifications of galaxy morphologies from the Galaxy Zoo 2¹ (GZ2) citizen science project (?), which obtains multiple independent classifications for each optical image. The full question tree for an image is shown in Figure 1 of ?. The GZ2 project used 304,022 images from the Sloan Digital Sky Survey Data Release 7 (SDSS; York et al. 2000; ?) all classified by *at least* 17 independent users, with a mean number of classifications of ~ 42 .

Further to this, we required NUV photometry from the GALEX survey (?), within which $\sim 42\%$ of the GZ2 sample was observed, giving 126,316 galaxies total ($0.01 < z <$

0.25). This will be referred to as the GZ2-GALEX sample. The completeness of this sample ($-22 < M_u < -15$) is shown in Figure 2 of Smethurst et al. (2015).

Observed fluxes are corrected for galactic extinction (Oh et al. 2011) by applying the ? law. We also adopt k -corrections to $z = 0.0$ and obtain absolute magnitudes from the NYU-VAGC (??).

2.2 Group Identification

We used the Berlind et al. (2006) catalogue, which uses a friends-of-friends algorithm to identify group and cluster galaxies in the SDSS. This was cross matched to the GZ-GALEX sample and limited to $z < 0.1$ to ensure GALEX completeness of the red sequence (see ?). Centrals were selected as the brightest galaxy in a group and all others were designated as satellites. This resulted in a sample of 14,199 group galaxies with 3,468 centrals and 10,731 satellites within a projected cluster centric radius range of $0 < R/R_{200} < 25$ and $z < 0.084$. This will be referred to as the GZ-GROUP sample.

2.3 Field sample

For all galaxies in the GZ-GALEX sample, we calculated the smallest projected cluster centric radii from each of the central galaxies in the Berlind et al. (2006) catalog and selected candidate field galaxies as those with (i) $R/R_{200} > 25$ and (ii) $\log \Sigma < -0.8$ from ?. This sample of field galaxy candidates was then matched in redshift and stellar mass to the central galaxies of the GZ-GROUP sample to give 2,309 field galaxies with $z < 0.084$. This will be referred to as the GZ-FIELD sample.

2.4 Deriving quenching parameters

STARPY² is a PYTHON code which allows the user to derive the quenching star formation history (SFH) of a single galaxy through a Bayesian Markov Chain Monte Carlo method (?)³ with the input of the observed $u - r$ and

^{*} This investigation has been made possible by the participation of over 350,000 users in the Galaxy Zoo project. Their contributions are acknowledged at <http://authors.galaxyzoo.org>

¹ <http://zoo2.galaxyzoo.org/>

² Publicly available: <http://github.com/zoouniverse/starpy>

³ <http://dan.iel.fm/emcee/>

$NUV - u$ colours, a redshift, and the use of the stellar population models of Bruzual & Charlot (2003). These models are implemented using solar metallicity (varying this does not substantially affect these results; ?) and a Chabrier IMF (?) but does not model for intrinsic dust. The SFH is modelled as an exponential decline of the SFR described by two parameters $[t_q, \tau]$, where t_q is the time at the onset of quenching [Gyr] and τ is the exponential rate at which quenching occurs [Gyr]. Under the simplifying assumption that all galaxies formed at $t = 0$ Gyr with an initial burst of star formation, the SFH can be described as:

$$SFR = \begin{cases} i_{sfr}(t_q) & \text{if } t < t_q \\ i_{sfr}(t_q) \times \exp\left(\frac{-(t-t_q)}{\tau}\right) & \text{if } t > t_q \end{cases} \quad (1)$$

where i_{sfr} is an initial constant star formation rate dependent on t_q (Schawinski et al. 2014; Smethurst et al. 2015). A smaller τ value corresponds to a rapid quench, whereas a larger τ value corresponds to a slower quench. We note that a galaxy undergoing a slow quench is not necessarily quiescent by the time of observation. Similarly, despite a rapid quenching rate, star formation in a galaxy may still be ongoing at very low rates, rather than being fully quenched. This SFH model has previously been shown to appropriately characterise quenching galaxies (Schawinski et al. 2014). We note also that star forming galaxies in this regime are fit by a constant SFR with a $t_q \simeq \text{Age}(z)$, (i.e. the age of the Universe at the galaxy’s observed redshift) with a very low probability.

The probabilistic fitting methods to these star formation histories for an observed galaxy are described in full detail in Section 3.2 of Smethurst et al. (2015), wherein the STARPY code was used to characterise the SFHs of each galaxy in the GZ2-GALEX sample. We assume a flat prior on all the model parameters and the difference between the observed and predicted $u - r$ and $NUV - u$ colours are modelled as independent realisations of a double Gaussian likelihood function (Equation 2 in Smethurst et al. 2015). We also make the simplifying assumption that the age of each galaxy, t_{age} corresponds to the age of the Universe at its observed redshift, t_{obs} .

The output of STARPY is probabilistic in nature and provides the posterior probability distribution across the two-parameter space for an individual galaxy the degeneracies for which can be seen in Figure 4 of Smethurst et al. (2015).

3 RESULTS

First start with a sanity check - do we reproduce morphology-density relation of Dressler 1980? Figure 1 shows the mean disc and smooth vote fractions from galaxy zoo, binned in projected cluster centric radius (normalised by the approximate virial radius of each group, R_{200}). We can see that the mean disc (smooth) vote fraction decreases (increases) from the mean field value (blue line) past 1 virial radius.

Figure 2 shows how the bar fraction (number of barred disc galaxies over the number of disc galaxies) increases towards the centre of the group population suggesting the possibility that the environment may play a role in triggering the disk instabilities which produce a morphological bar (???).

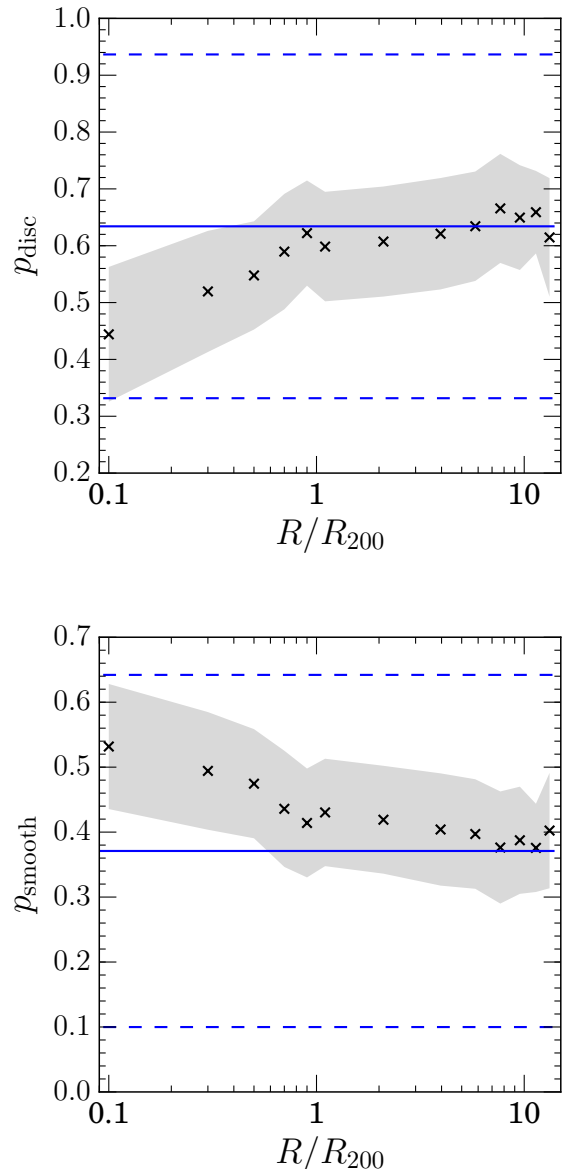


Figure 1. Mean GZ vote fraction for disc (top) and smooth (bottom) galaxies in the GZ-GROUP sample binned in projected cluster centric radius, normalised by R_{200} , a proxy for the virial radius of a group. The mean vote fractions of the FIELD sample are shown (blue solid lines) with $\pm 1\sigma$ (blue dashed lines).

Figure 3 shows how the merger fraction does not significantly deviate from the field fraction (blue line) until beyond 1 virial radius. Similarly in Figure 4 the left panel shows how those galaxies identified as having no or just noticeable bulges are less common in the inner regions of the cluster (left panel), whereas the fraction of galaxies with obvious or dominant bulges (thought to be grown by mergers;???) increases with decreasing projected distance from the centre of the cluster

Figure 5 shows how the SFR of the GZ-GROUP sample declines with decreasing cluster centric distance, significantly below the mean SFR of the GZ-FIELD sample shown by the blue dashed line. This is in agreement with the re-

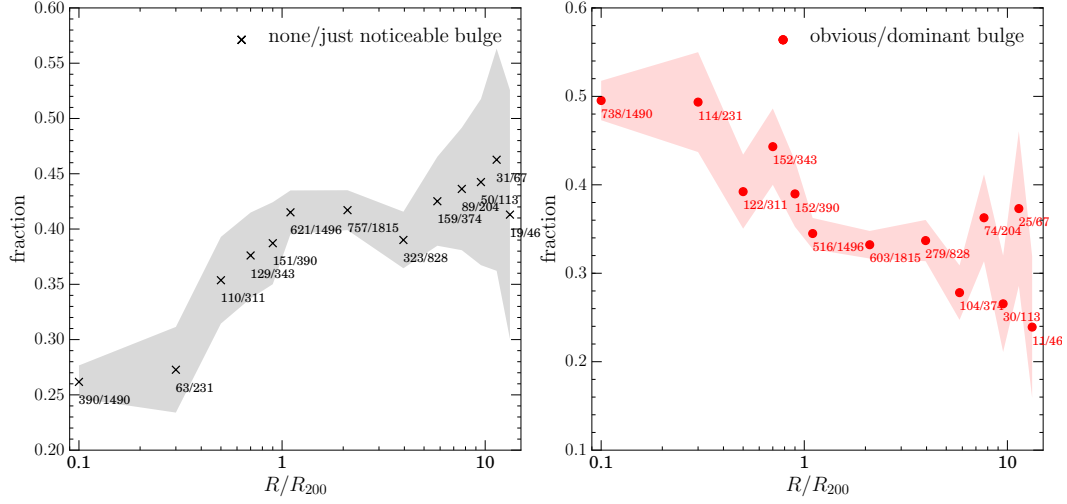


Figure 4. Fraction of galaxies with none/just noticeable bulge classifications (left) and with obvious/dominant bulge classifications (right) in the GZ-GROUP sample binned in projected cluster centric radius, normalised by R_{200} , a proxy for the virial radius of a group.

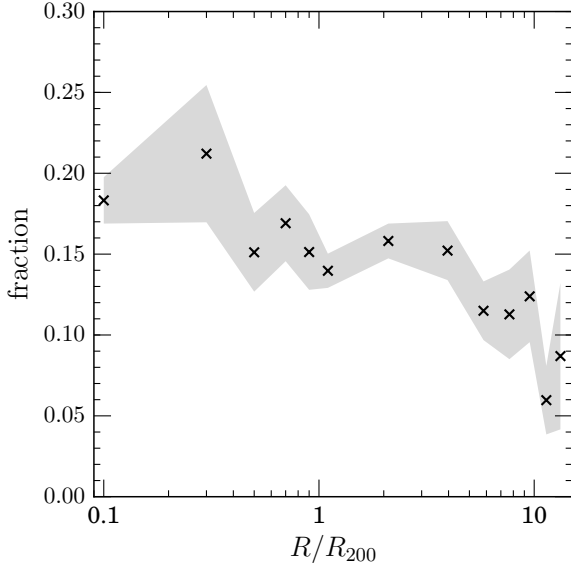


Figure 2. Bar fraction (number of barred disc galaxies over number of disc galaxies) in the GZ-GROUP sample binned in projected cluster centric radius, normalised by R_{200} , a proxy for the virial radius of a group.

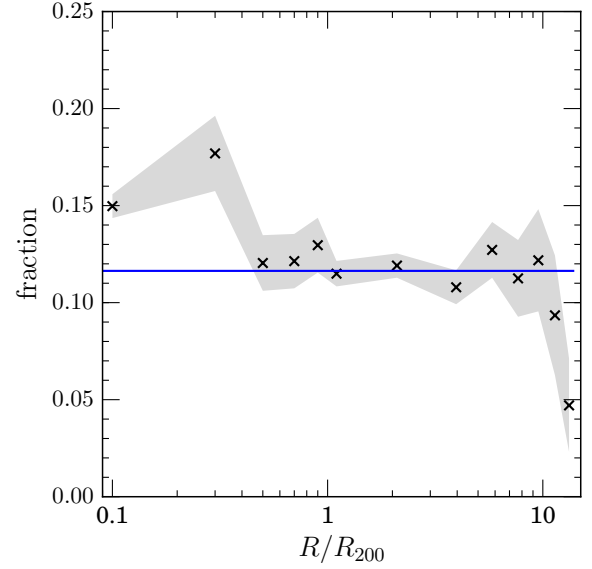


Figure 3. Merger fraction in the GZ-GROUP sample binned in projected cluster centric radius, normalised by R_{200} , a proxy for the virial radius of a group. The mean merger fraction of the FIELD sample is shown by the blue solid line.

sults of Gómez et al. (2003) who observe the decline in SFR with cluster centric radius in SDSS clusters (see for example, Figure 6 in Gómez et al. 2003).

With the results from STARPY we can look at the time since quenching onset ($\Delta t = t_{\text{obs}} - t_{\text{quench}}$, see Section ??) binned in projected cluster centric radius, normalised by R_{200} (a proxy for virial radius) for satellite galaxies and central galaxies in the GZ-GROUP sample, compared with galaxies in the GZ-FIELD sample. We can investigate these trends with group properties as shown in Figures 6 & 7.

4 DISCUSSION

5 CONCLUSIONS

REFERENCES

- Berlind A. A. et al., 2006, ApJS, 167, 1
- Bruzual G., Charlot S., 2003, MNRAS, 344, 1000
- Dressler A., 1980, ApJ, 236, 351
- Gómez P. L. et al., 2003, ApJ, 584, 210
- Oh K., Sarzi M., Schawinski K., Yi S. K., 2011, ApJS, 195, 13
- Schawinski K. et al., 2014, MNRAS, 440, 889

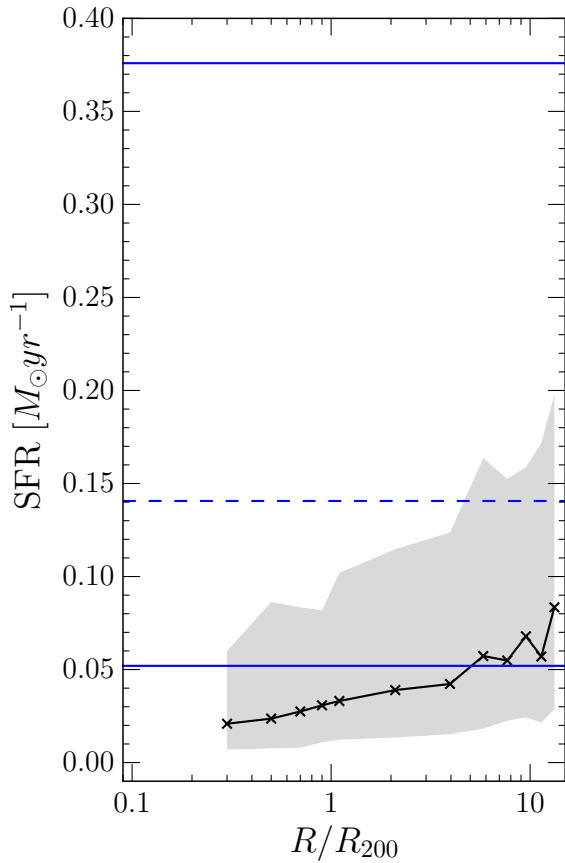


Figure 5. $H\alpha$ derived star formation rates in the GZ-GROUP sample binned in projected cluster centric radius, normalised by R_{200} , a proxy for the virial radius of a group. The mean SFR of the FIELD sample is shown (blue dashed line) with $\pm 1\sigma$ (blue solid lines).

Smethurst R. J. et al., 2015, MNRAS, 450, 435
York D. G. et al., 2000, AJ, 120, 1579

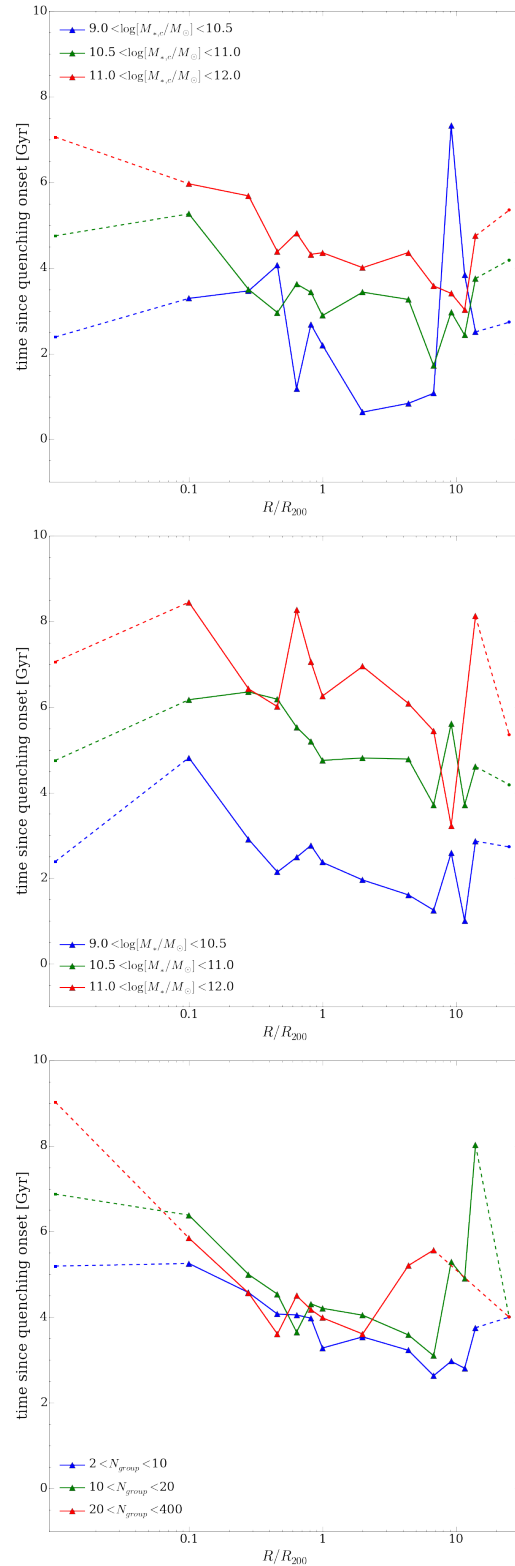


Figure 6. The time since quenching onset ($\Delta t = t_{obs} - t_{quench}$) binned in projected cluster centric radius, normalised by R_{200} , for satellite galaxies (triangles) split by stellar mass of the corresponding central galaxy (top), stellar mass (middle) and the number of galaxies within the group (bottom). The corresponding values for central galaxies (squares) and field galaxies (circles) are shown and connected by the dashed lines to aid the reader.

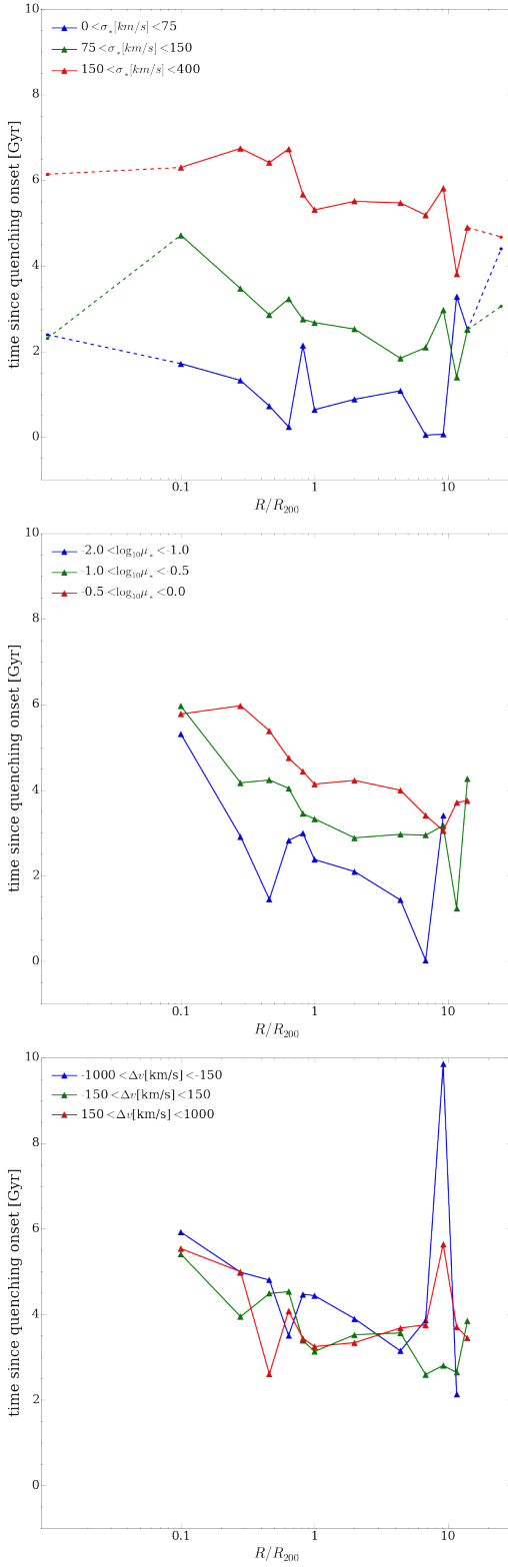


Figure 7. The time since quenching onset ($\Delta t = t_{\text{obs}} - t_{\text{quench}}$) binned in projected cluster centric radius, normalised by R_{200} , for satellite galaxies (triangles) split by velocity dispersion (top), stellar mass ratio ($\mu_* = M_*/M_{*,c}$) (middle) and the difference in velocity from the associated central galaxy (bottom). The corresponding values for central galaxies (squares) and field galaxies (circles) are shown and connected by the dashed lines to aid the reader in the top panel where appropriate.